Production of fat-based emulsion powder by prilling process using twin-fluid atomizer for controlled release of iron

Bipro N. Dubey*, Erich J. Windhab
Lab. of Food Process Engineering, Department of Health Science and Technology (D-HEST),
ETH Zurich, Switzerland.
bipro.dubey@hest.ethz.ch and erich.windhab@hest.ethz.ch

Abstract

Encapsulation of iron is necessary to supply bioavailable iron to large number of population possess iron deficiency. In the present study, we dispersed the iron solution in a fat matrix of palm stearin, and prepared the simple emulsion (water-in-oil) at $60\,^{\circ}\mathrm{C}$, where fat was a continuous phase. Using that emulsion, we produced fat based emulsion particles through prilling (spray + chilling) process using twin fluid atomizers (internal mixing). We characterized the particle in terms of size and size distribution, and investigated the internal structure of the fat-particles by cryogenic scanning electron microscopy (cryo-SEM) for observing the distribution or homogeneity of dispersed phase. Present study includes mainly the iron release kinetics through the fat matrix of the emulsion particle in an in-vitro gastric system ($pH \approx 2.0$) as a function of (a) particle size of prills, (b) thickener concentration (polyethylene glycol, PEG) in dispersed phase, (c) droplet size of dispersed phase, (d) mixing properties (Reynolds number, *Re*), and (e) shelf-life of particles. The release kinetics was explained by the second order kinetics, where we estimated the release kinetic constant, and co-related with the viscosity ratio of dispersed phase to continuous phase, mean particle size of emulsion, and shelf-life of particles. The result showed that the control of the release properties can be obtained by choosing particle size and thickener concentration.

Introduction

Emulsions are consisting of a dispersed phase (commonly as a droplet) in an immiscible liquid so-called continuous phase. The dispersed phase can be either droplets of a single liquid (in the case of simple emulsion), or an emulsion (in the case of a double or multiple emulsion). Emulsions are usually used for encapsulation of functional components due to their hydrophilic or lipophilic cores. The hydrophilic or lipophilic cores/layers of emulsions give the opportunity to enclose a polar or non-polar component for the application of encapsulation. Moreover, the lipophilic layer does not allow the hydrophilic component to migrate outside easily or vice versa. However, emulsions are less stable in liquid form in terms of long shelf-life as well as during intended application. Therefore, the microstructure of emulsion is a dynamically changing property that is also an indication of undesirable time dependent changes of the encapsulation capacity. Many researchers had worked to improve the stability of emulsions. Powder formation from emulsion would be a technological solution in this regard. The reason is that the solid particle of emulsion will have greater stability compared to that of pre-emulsion. Spray drying or spray-chilling/cooling can be used to produce large-scale production of particle from emulsion. Both processes are an integrated process of atomization with drying/chilling. Therefore, for understanding of spray-chilling or drying, atomization of emulsion has to be significantly studied in a first place [1, 2, 3, 4]. Some authors [5, 6] studied spraying of emulsion, where they investigated the influences of process condition and viscosity of emulsion on the spray droplets as well as the spraying impact on the microstructure of emulsion.

The aims of the present study are (i) the encapsulation of iron in a dispersed phase of a fat-based emulsion, (ii) production of solid particle (prills) out of the emulsion and characterization of the particle (in terms of shape, size and size distribution), (iii) to investigate the microstructure of the prills to observe the homogeneity of dispersed phase, as well as the shape and size of the dispersed droplet, and most importantly (iv) the release kinetics of iron in a gastric condition (acidic solution of pH $\approx$ 2.0). The release of iron from the prills is well exhibited by second order kinetics. A simplified model is implemented for fitting the experimental data, and correspondingly the release kinetics rate constant has been calculated. The experimental result shows that the release kinetics rate constant is a function of particle size, viscosity ratio of dispersed to continuous phase (which is an indication of droplet size of dispersed phase). Therefore, a controlled release properties of iron (encapsulated in fat-based emulsion prills) can be achieved by choosing respective particle size and droplet size of dispersed phase.

*Corresponding author: bipro.dubey@hest.ethz.ch, Phone: +41 44 63 28 559

Table 1. Composition of emulsion and its corresponding particle size

Name of emulsion	Emulsion Types	Composition of continuous phase	Composition of dispersed phase	Name of sample	$X_{50,3}$, μm
A	40 W/O	1.9 %wt span-20, 2.86 %wt PGPR in palm stearin	16.4 %wt PEG, 16 gm $FeSO_4$ in 0.01 M HCl	A1	374 ± 21
				A2	130 ± 12
				A3	85 ± 2.0
				A4	55 ± 2.0
				A5	44 ± 1.0
E	40 W/O	1.9 %wt span-20, 2.86 %wt PGPR in palm stearin	22.7 %wt PEG, 16 gm $FeSO_4$ in 0.01 M HCl	E1	517 ± 12
				E2	276 ± 6.0
				E3	101 ± 2.0
				E4	59 ± 1.0
				E5	43 ± 1.0
F	40 W/O	1.9 %wt span-20, 2.86 %wt PGPR in palm stearin	28.2 %wt PEG, 16 gm $FeSO_4$ in 0.01 M HCl	F1	630 ± 3.0
				F2	386 ± 10
				F3	106 ± 3.0
				F4	59 ± 0.5
				F5	47± 1.0

Materials and Methods

Materials

The continuous phase of the emulsion (approx. 40 % water-in-oil, W/O) is palm stearin (Florin AG.), which contains 1.9 %wt Span-20 (Sorbitan monododecanoate, Fluka, Switzerland) as emulsifier and 2.86 %wt PGPR (poly-glycerol polyricinoleate, DANISCO, Denmark) as stabilizer as well as emulsifier. The dispersed phase of the emulsion (water-in-oil, W/O) is iron solution (constant amount, 16 mg, of $FeSO_4$ in a 0.01 M HCl solution, pH $\approx$ 2.0) that contains 16.4, 22.7 or 28.2 %wt of PEG (Polyethylene Glycol, $M_w \approx 35$ kDa; Clariant, Switzerland) as thickener (viscosity modifier), which could also influence the release kinetics of iron in gastric condition. The composition of three different types of emulsions as will be mentioned in this article, are given in detail in Table 1.

Preparation and characterization of emulsion

Simple emulsion (W/O) is prepared by rotor-stator device (Polytron PT6000, Kinematica AG) at very high rotational speed (about to 7000 rpm) for 30 min at constant temperature (60 °C). We assume that this long term acting high rotational speed leads to an equilibrium mean droplet size of the dispersed phase. In general, the droplet size is found to be about 1 to 4 μm depending on the viscosity of dispersed phase at the given rotational speed, which is also confirmed by cryo-SEM investigation of prills. Due to low stability of fat based emulsion at high temperature, the emulsions are used in prilling experiment immediately after preparation. The shear rate dependent viscosities of the dispersed and continuous phase of emulsion samples are measured using shear rheometer (Anton Paar, Physica MCR 300, Couette geometry, measuring gap 1.13 mm).

Prilling experiment

A prilling tower (height is about 4.5 m, and diameter is 1 m) is used for the production of solid particle out of emulsions. Two different types of twin-fluid nozzle geometries (Internal & External mixing) are used for the experimental investigations. Experimental results of prilling using internal mixing nozzle (INMIX) are only reported here for simplicity. The emulsions are treated by the GLR (gas-liquid mass ratio) of 0.282 (1), 0.376 (2), 0.724 (3), 0.939 (4), and 1.377 (5) at constant liquid flow (138 ml/min) for INMIX (average temperature inside the tower is about -10 °C). Particle is collected from the bottom of the tower and stored in room temperature in a closed container. The corresponding particle sizes of three different types of emulsions are also reported in Table

1.

Characterization of particle

The direct and qualitative observation of the emulsion-particles is carried out by the inverse light microscopy (max. mag. 60x; Nikon AG.) and cryo- scanning electron microscopy (SEM). The size and size distribution of the particles are also studied by the Laser Diffraction Particle Size Analyzer, LDPSA (LS 13320, Beckman Coulter, Inc.) applying the Fraunhofer model for more precise values compared to microscopy picture. Internal microstructure of the particles are also investigated by cryo-SEM after cutting the sample in the low temperature sample preparation steps.

Iron release experiment

40 gm of iron encapsulated emulsion particles are dispersed in 800 ml in-vitro gastric solution (0.01 HCl, pH $\approx$ 2.0, initial concentration of iron $C(t=0) = 0$ ppm). The particles are stabilized by adding $\approx$ 1 ml of Tween-20 (Polysorbate 20). An impeller type of stirrer is used for mixing the solution homogeneously and the stirring rate is varied from 50 to 200 rpm to investigate the impact of stirring rates on the release kinetics. Complete dispersion of the particles into the solution takes approximately 1-5 min depending on the size of particles (though time count starts from the first contact of particle into gastric solution), and then the sampling of iron solution is taken time to time for maximum time of 30 hrs. The sample is diluted, and the iron content is measured using atomic absorption spectroscopy (AAS).

Theory of release properties

Initial concentration of in-vitro gastric solution has a value of $C_0 \approx 0$ ppm. During stirring of particle into the gastric solution, the concentration, C(t), increases over time, and finally can reach to an equilibrium value, C_∞ (the maximum possible concentration). The release properties show a second order kinetics that can be expressed by the following differential equation (1).

$$\frac{dq(t)}{dt} = k(q_\infty - q)^2 \tag{1}$$

where, $C(t)$ is a concentration at time t; $q(t) = C(t)/C_\infty(t=\infty)$, q_∞=$C_\infty/C_\infty \approx 1$, and k is the release kinetic constant, which is a specific release property of a distinct particle. The above equation (1) can be analytically solved by integrating over a range of time from $t = 0(q = 0)$ to $t(q(t))$. The final equation can be rearranged and expressed as follows (equation 2):

$$q = \frac{q_\infty^2 kt}{1 + q_\infty kt} \tag{2}$$

when t tends to zero, $(1 + q_\infty kt) \approx 1$ and $q = q_\infty^2 kt$, where $q_\infty^2 k$ is the initial release rate. On the other hand, the above equation (2) can be represented as follows, which is similar to the Langmuir type equation (3).

$$q = q_\infty \frac{q_\infty kt}{1 + q_\infty kt} \tag{3}$$

where $q_\infty k$ is an equilibrium constant. The above equation can be rearranged and obtained a linear relationship of t/q as a function of t.

$$\frac{t}{q} = \frac{1}{q_\infty^2 k} + \frac{t}{q_\infty} \tag{4}$$

Since $q_\infty \approx 1$, the above equation (4) can be simplified as the following equation (5),

$$\frac{1}{q} = \frac{1}{kt} + 1 \tag{5}$$

where k is a release rate constant as well as very close value to the equilibrium constant of iron release. Final equation for the release rate can be expressed by the equation (6).

$$q = \frac{kt}{1 + kt} \tag{6}$$

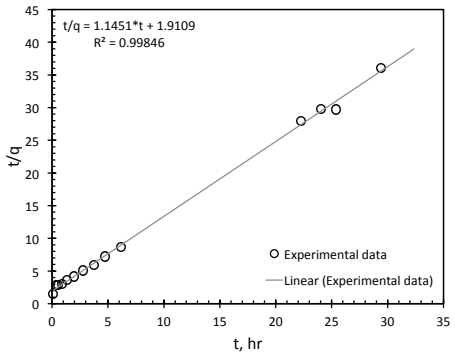

Figure 1. According to equation (4), t/q has been plotted as a function of t (sample A5) for getting information about q_∞ and k.

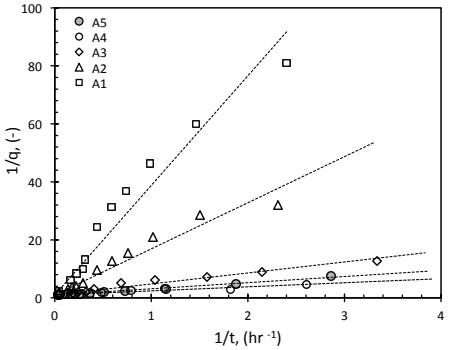

Figure 2. For getting information on release kinetic rate constant k (Table 2) of all samples of A, 1/q has been plotted as a function of 1/t. A linear relationship is found as shown in equation (5).

Table 2. The release kinetic rate constants for different emulsion particles

Samples	A1	A2	A3	A4	A5	E1	F1	F2	F5
k, hr^{-1} (after 1 week)	0.0259	0.0629	0.2645	0.5260	0.4722	2.9061	0.0667	0.2660	2.7210
k, hr^{-1} (after 4 weeks)	0.0539	-	-	-	0.5178	-	-	-	-

Results and Discussion

Model equation and iron release kinetics

From the equation (4), t/q is plotted (Figure 1) as a function of t for a sample named A5 (Table 1). The results nicely show a linear relationship and the slope value gives $1/q_\infty$ ($q_\infty = 0.87$) and corresponding $k = 0.6862$ hr^{-1} (observation time approximately 30 hr). It shows that the concentration value will never meet the maximum possible concentration (C_∞), which is theoretically not accurate. Therefore, we assume that $q(t)$ will be $q_\infty \approx 1$ at very large time of mixing. So, the equations (3) and (4) become much simpler as given by the equations (6) and (5) respectively. The release behavior of particles with different mean size has been plotted in Figure 2, where $1/q$ as a function of $1/t$ (equation 5). It is seen that the experimental results are in good agreement with the model equation (5).

The release kinetic rate constant for sample A5 is found to be 0.4722 hr^{-1}. In the similar way, the release kinetics of other samples of prills (as listed in Table 1) are calculated and the values are given in Table 2.

Influence of GLR on particle size using INMIX nozzle

Prilling (spraying + chilling) process is used for producing particle from three different emulsion samples (Table 1). The mean diameter $X_{50,3}$ of the particle is plotted as a function of GLR in Figure 3. The figure also shows the corresponding Span (($X_{90,3}$-$X_{10,3}$)/$X_{50,3}$). The result shows that the mean particle size is decreasing with increasing GLR for all emulsions. It is also seen that the mean particle size is higher at a given GLR for the emulsion with higher viscosity (due to higher viscous dispersed phase). The particle size distribution of the two emulsions (A and F) are given in Figure 4, which shows that the particle size of emulsion F is relatively higher than that of emulsion A. Whereas the higher GLR condition give similar size distribution and mean particle size for both emulsions. Because, at higher GLR, the impact of aerodynamic force is much higher compared to the viscous force. Therefore, viscosity of the sample is not influencing much on the particle size.

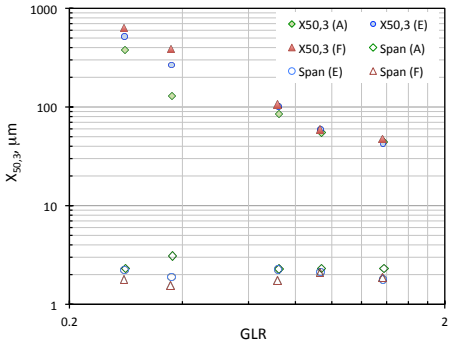

Figure 3. Mean particle sizes of three different types of emulsions are shown as a function of GLR and corresponding Span values are also reported.

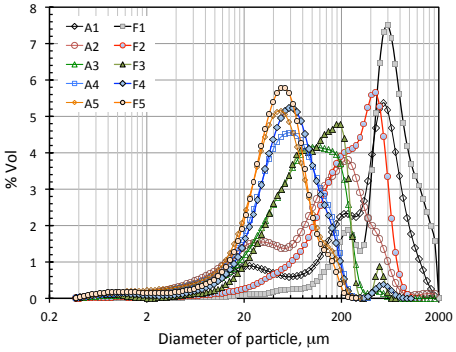

Figure 4. Size distribution of the particles (corresponding mean particle size as shown in Figure 3) of emulsion A and F are plotted as a function of particle diameter, d.

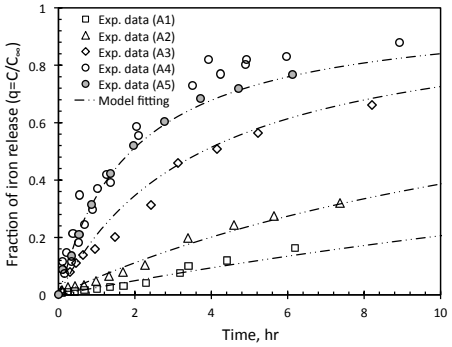

Figure 5. Fraction of iron release of emulsion A as a function of time (up to 10 hr), where the dotted lines are model fitting and symbols are the experimental data.

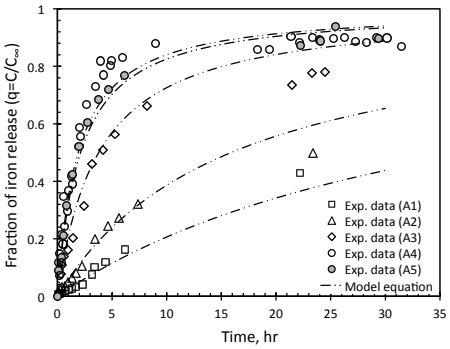

Figure 6. Fraction of iron release of emulsion A as a function of time (up to 30 hr), where the dotted lines are model fitting and symbols are the experimental data.

Influence of particle size on iron release kinetics

In Figures 5 to 8, it is seen that the release properties of iron for two different emulsions (A and F) varied depending on the particle size. In Figure 5, the iron release kinetics of emulsion particle A is plotted as a function of time (up to 10 hr) where experimental data (symbols) is well represented by the second order kinetic model equation (dashed lines). It is found that the smaller particles exhibit faster release kinetics compared to that of the bigger particles, because the smaller particles have higher surface to volume ratio than the bigger particles. It is also seen that the prediction by the model equation is well fitted with the experimental data in the shorter time range (up to10 hr) whereas a little discrepancy is seen for the longer time range (up to 30 hr) as shown in Figure 6. The similar trend is also found for the emulsion F as shown in Figures 7 and 8.

PEG in dispersed phase and its influence on release kinetics

Three different types of emulsions are used where only variation is maintained in the thickener composition (16.4, 22.7, 28.2 %wt PEG) in dispersed phase. In Figure 4, it is already seen that the particles (A5 and F5) produced at highest GLR are showing nearly same size distribution. Therefore, iron release experiments using those particles are carried out while varying PEG concentration in dispersed phase. The results depict that the lower PEG contained particles show lower release kinetics compared to that of the higher PEG contained particles (Figure 9). Here again, the model can well predict the experimental data even at the longer time range (Figures 9 and 10). However, the particles containing 22.7 %wt and 28.2 %wt PEG do not show significant difference on release kinetics. The viscosity ratio of dispersed to continuous phase is much higher which correspondingly lead to bigger droplets compared to the particles with lower PEG. In addition, the dispersed drop size might be different

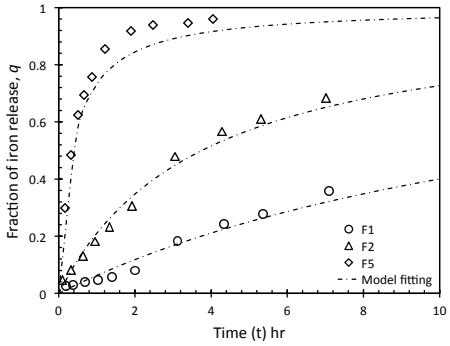

Figure 7. Iron release kinetics of emulsion F as a function of time (up to 10 hr), where the dotted lines are model fitting and symbols are the experimental data.

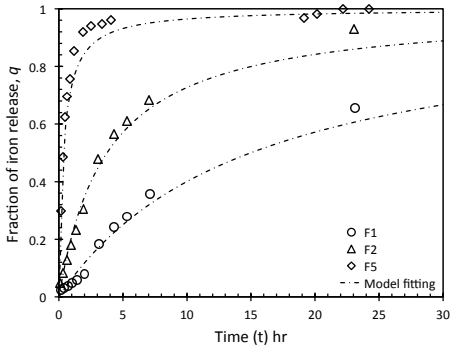

Figure 8. Iron release kinetics of emulsion F as a function of time (up to 30 hr), where the dotted lines are model fitting and symbols are the experimental data.

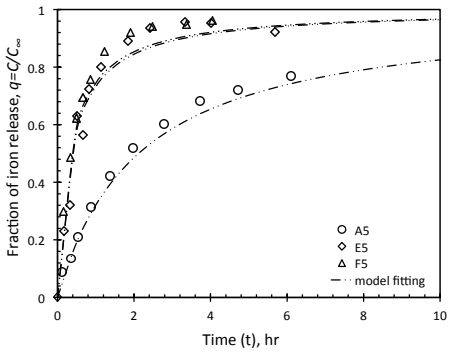

Figure 9. Influence of PEG concentration in dispersed phase on iron release kinetics as a function of time (up to 10 hr). The particle size distribution of the samples A5, E5 and F5 is the same as in Figure 4.

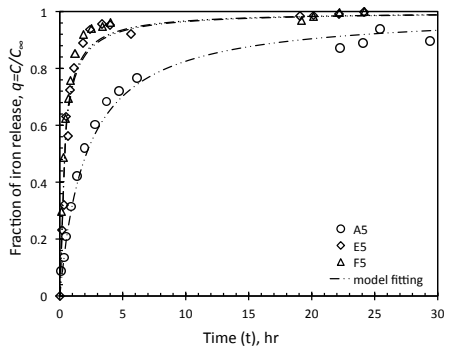

Figure 10. Influence of PEG concentration in dispersed phase on iron release kinetics as a function of time (up to 30 hr). The particle size distribution of the samples A5, E5 and F5 is the same as in Figure 4.

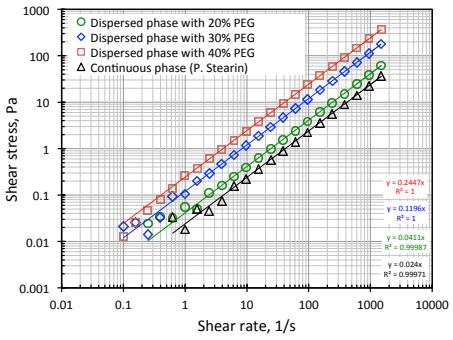

Figure 11. Shear stress as a function of shear rate of dispersed and continuous phase at 60 °C.

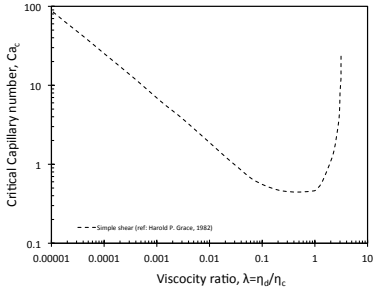

Figure 12. The critical capillary number as function of viscosity ratio of dispersed to continuous phase. The figure is regenerated from [10]

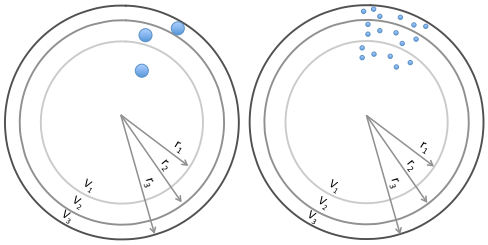

Figure 13. Schematic representation of three different area layers of a spherical particle with equal volume (V_1 = V_2 = V_3).

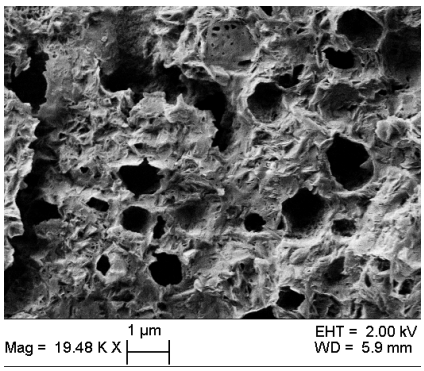

Figure 14. Internal cross-sectional image of sample A1 by cryo-SEM.

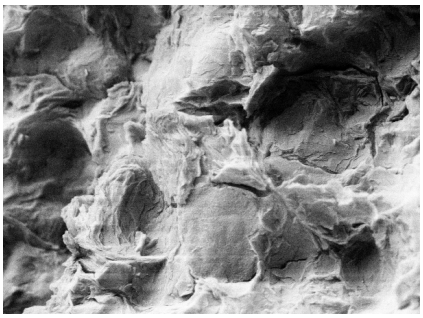

Figure 15. Internal cross-sectional image of sample F1 by cryo-SEM and scale of the picture is same as Figure 14.

due to the different critical capillary number (a function of viscosity ratio) at a given dispersing energy input. The viscosity data of dispersed and continuous phase is represented in Figure 11. The ratios are 1.7, 5 and 10 for three different emulsions containing 16.4, 22.7, 28.2 %wt of PEG in dispersed phase respectively. In Figure 12, it is seen that the smaller droplets are only found in very close value of the the viscosity ratio of dispersed to continuous phase equal to one. Therefore, the droplets of dispersed phase with 16.4 %wt PEG is much smaller compared to the other two emulsions (with higher PEG). In contrast, the PEG concentration of 22.7 and 28.2 %wt in dispersed phase leads to very large emulsion droplets and showing very fast release kinetics which is not easy to differentiate. In Figure 13, one circle has been divided into three equal volume ($V_1 = V_2 = V_3$) surface area, where the radius are in a relation as r_3 = 1.2599 r_2 = 1.442 r_1. Therefore, one big droplet in a given volume will have faster release compared to smaller drop distributed in equal volume as shown in Figure 13. The bigger droplet size of dispersed phase of emulsion F has been confirmed by cryo-SEM, and compared to the droplet size of dispersed phase of emulsion A (as shown in Figures 14 and 15). The dispersed phase drop size of sample F1 is about more than three times larger than the droplet of A1. In both cases, droplets of the dispersed phase are evenly distributed.

Impact of mixing phenomena and shelf-life of particle on release kinetics

The mixing properties are usually characterized by Reynolds number (Re) that can be defined by equation (7)

$$Re = \frac{\rho N d^2}{\eta} \tag{7}$$

where, density, $\rho \approx 1000\ kg/m^3$; diameter of impeller, d = 0.06 m; stirring rates, N = 50, 100, 200 rpm; and viscosity of suspension, η = 1 mPa.s.

The result shows that the mixing does not have much impact on the release kinetics in the observation range of stirring (50-200 rpm) as shown in Figure 16. The reason could be that the investigated stirring rate (50-200 rpm) is already high enough (corresponding Re $\approx 2\times10^3$ to 8.3×10^3) to mix the solution very homogeneously, therefore, there is no chance to have some resistance due to the mixing phenomenon. In Figure 16, the fraction of iron release (sample A1 and A5) is plotted as a function of time (up to 30 hr), where the release properties of smaller

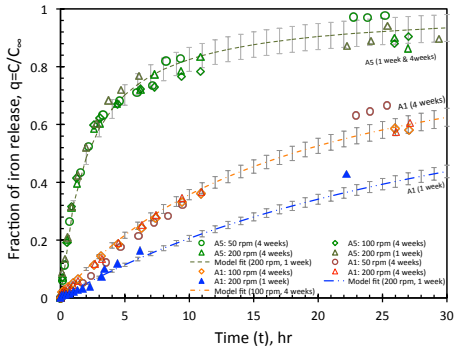

Figure 16. Influence of mixing properties and shelf-life on iron release kinetics of sample A1 and A5 as a function of time (up to 30 hr).

particles are not significantly changed depending upon shelf-life from 1 to 4 weeks. Whereas, the release kinetics of bigger particles is changed during 4 weeks storage time compared to 1 week storage. Larger deformation of bigger particles due to fast freezing during prilling causes larger fracture compared to smaller particles. Therefore, the release kinetics of larger particle (A1) is much influenced by the shelf life. On the other hand, smaller particles have smoother surface than the bigger particles, which denote a longer shelf life.

Conclusions

Prilling is a suitable process technology for production of fat based emulsion particles for nutrient encapsulation purposes. The iron release from the emulsion fat-matrix can be well controlled by choosing the particle size and droplet-size of dispersed phase. The release kinetics of iron follows a second order kinetics. Whereas, the iron release kinetics from a smaller particle is higher compared to a bigger particle due to larger specific surface to volume ratio. The iron release kinetics of a particle having bigger droplet in dispersed phase is found to be higher compared to that of a smaller droplet. In addition, the shelf-life also has much influences on release kinetics of the larger particle.

Acknowledgements

We would like to thank to German research foundation (DFG) for financial support under the DFG-Schwerpunktprogramm (SPP)-1423 program. We would also like to thank to Electron Microscopy Center of ETH Zurich (EMEZ) and Lab of Human Nutrition (IFNH, ETH Zurich) for giving opportunity to use cryo-SEM instrument and AAS equipment respectively.

References

[1] Dubey, B. N., Duxenneuner, M. R., Windhab, E. J., *Proc. 23th European Conference on Liquid Atomization and Spray Systems, Brno, Czech Republic*, 2010.
[2] Dubey, B. N., Duxenneuner, M. R., Windhab, E. J., *Proc.11th International Congress On Engineering and Food, Athens, Greece*, 2011.
[3] Dumouchel, C., *Experiment in Fluids* 45: 371-422 (2008).
[4] Walzel, P., *Ullmann's Encyclopedia of Industrial Chemistry* Wiley-VCH Verlag GmbH & Co. KGaA 2010.
[5] Bolszo, C. D., Narvaez, A. A., McDonell, V. G., Dunn-Rankin, D. and Sirignano, W. A., *Atomization and Sprays* 20 (12):1077-99 (2009).
[6] Dubey, B. N., Duxenneuner, M. R., Windhab, E. J., *Proc. 24th European Conference on Liquid Atomization and Spray Systems, Estoril, Portugal*, 2011.
[7] Zimmermann, M. B., Windhab, E. J., *Encapsulation Technology for Active Food Ingredients and Food Processing (chapter-7),* Eds. N. J. Zuidam and V. A. Nedovic, Springer Science+Business Media 2010.
[8] Theil, E. C., *Annu. Rev. Nutr.* 24: 327-43 (2004).
[9] Gaudio, P. D., Colombo, P., Colombo, G., Russo, P., Sonvico, F., *International Journal of Pharmaceutics* 302: 1-9 (2005).
[10] Grace, H. P., *Chemical Engineering Communications* 14: 225-277 (1982).